数理解析研究所講究録
第1735巻 2011年 198-212

A Halo Current and Magnetic Field of a Permanent Nut-shaped Magnet

Haiduke Sarafian
The Pennsylvania State University
University College
York, PA 17403

Abstract

A magnetic field of a nut-shaped permanent magnet along the axial symmetry axis perpendicular to the plane of the nut through its center is measured. Theoretical models based on various electrical current distributions within the magnet have been proposed to account for the field. However, conventional current distributions result in a misalignment between data and the conventional theoretical models. The issue is rectified by proposing the existence of a non-conventional, displaced current in the region beyond the outer physical boundary of the nut. The displaced current resembles a *halo* around the magnet. The parametrization of the *halo* current leads to a perfect match between data and the model. The computational and graphical challenges including various animations all are addressed with the latest version of *Mathematica*.

Keywords : Magnetic field of a permanent nut-shaped magnet, *halo* current, *Mathematica*

1 Introduction and motivation

In our previous analysis we investigate the features of a nonlinear oscillations of a pair of solid cylindrical permanent magnets [1]. In doing so we were in need of knowing the value of the magnetic moment of the individual magnet; two distinct empirical methods were practiced. The collected data were analyzed and a theoretical model was proposed to justifying the underlying features of the data. In short, the trust of the theoretical model was based on assuming the field along the axial symmetry axis of the cylinder through its center and its associated moment

are due to a uniform electric current distribution confined only to the outer surface of the cylinder. With this assumption we were able to interpret the data and deduce the field and the associated moment. As discussed in [1] the oscillating magnet stays apart from the stationary one. Its shortest distance of approach is long justifying the utilization of the proposed current distribution within the permanent magnet.

In the process of extending our analysis beyond the issues addressed in [1] instead of utilizing a cylindrical solid permanent magnet we utilized nut-shaped magnets. In our new experiments we were also in need of measuring the magnetic field and its associated magnetic moment not only at far distances along the axial symmetry axis but at close distances as well. Here, to focus on the issues at hand, in Fig 2 we display the collected data. This is a plot of magnetic field vs. distance from the center of the nut.

According to displayed data in Fig 2, the field vs. distance has two distinct features. The tail of the data, i.e. the strength of the field for distances far from the center falls off in proportion to the inverse distance to some power. The head of the data, i.e. the strength of the field for distances close to the center, however, deviates from interpolation of the latter. It is the objective of our study to understand and reason the features of the field. To accomplish this, our crafted work is composed of four sections. In addition to Introduction and objectives in the Experiment section, we outline the experiment setup. In the Analysis section after outlining the generalities of the magnetic field we detailed three progressive models conducive to the fourth successful one. The details of model 4 entails the *halo* current and shows its impact on evaluating field that is compatible with data. In the last section, we close our work making a few conclusive comments.

2 Experiment

We obtain a nut-shaped permanent magnet with specifications of the inside, outside radii and thickness of $\{R_1,\ R_2,\ t\} = \{0.5, 1.0, 0.3\}$cm. Web site [2] embodies a host of nut-shaped magnets with various specifications. The magnet used to measure the distance of the tip of the magnetometer to the center of the magnet. A photo of the set up is shown in Fig 1. Utilizing Pasco data acquisition Interface 750 [4] and Data Studio software [5] data was collected and stored. The collected data was stored in a spreadsheet format. To further the analysis the data was imported in *Mathematica* [6]. Follow-up numeric manipulations, graphs as well as symbolic calculations all are carried out deploying the latest version of *Mathematica*; V 7.01. The data is shown in Fig 2. These are the averaged values of the measurements that was repeatedly collected and tallied in a course of a few days.

```
image1 = Import[
   "C:\\DataFiles\\MagnetostaticSpringNonlinearOscillations_October_2009\\IMG_
     4266.JPG", ImageSize -> {300, 300}];

image2 = Import[
   "C:\\DataFiles\\MagnetostaticSpringNonlinearOscillations_October_2009\\IMG_
     4263.JPG", ImageSize -> {300, 300}];

GraphicsGrid[{{image1, image2}}, ImageSize → {600, 400}]
```

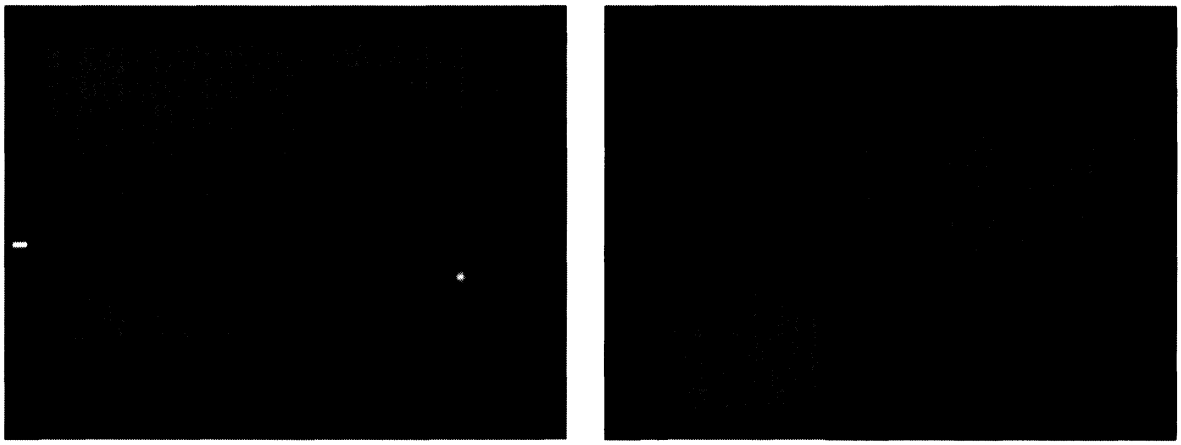

Figure 1. A nut-shaped permanent magnet, a magnetometer and a wooden ruler are in display (the left side photo). The right side photo is a snap shot of an instance of a registered magnetic field on the screen of a computer which is connected to the interface.

```
dataNutmagnetDec16 = {{2, {950}}, {4, {927}}, {5, {903, 908}}, {6, {835, 864}},
    {8, {678, 712, 688, 699}}, {10, {546, 561, 561, 551, 571}}, {12, {435}},
    {14, {395, 366, 383}}, {15, {348}}, {16, {327, 332}}, {18, {273, 270}},
    {20, {234, 234, 239, 241, 248}}, {22, {205, 224, 229, 234}}, {24, {177, 205}},
    {25, {185, 187}}, {26, {161, 170, 185}}, {28, {146, 156, 168, 177}},
    {30, {135, 141, 143, 148, 153}}, {32, {127, 151, 158}}, {34, {119}},
    {35, {133}}, {36, {114, 124}}, {38, {109, 131, 136, 138}},
    {40, {104, 109, 115, 115, 122}}, {46, {92}}, {50, {83, 114}}};

dataNutmagnetDec16 = dataNutmagnetDec16 /. {p_, q_} → {0.001 (p(*+6.5/2*)), q};

listplotdataNutmagnetDec16 =
 ListPlot[Table[{dataNutmagnetDec16[[i, 1]], Mean[dataNutmagnetDec16[[i, 2]]] // N},
   {i, 1, Length[dataNutmagnetDec16]}], GridLines → Automatic, PlotMarkers → {■},
  PlotRange → {{0, 0.04}, {0, 1000}}, AxesLabel → {"z,m", "B_field(gauss)"}]
```

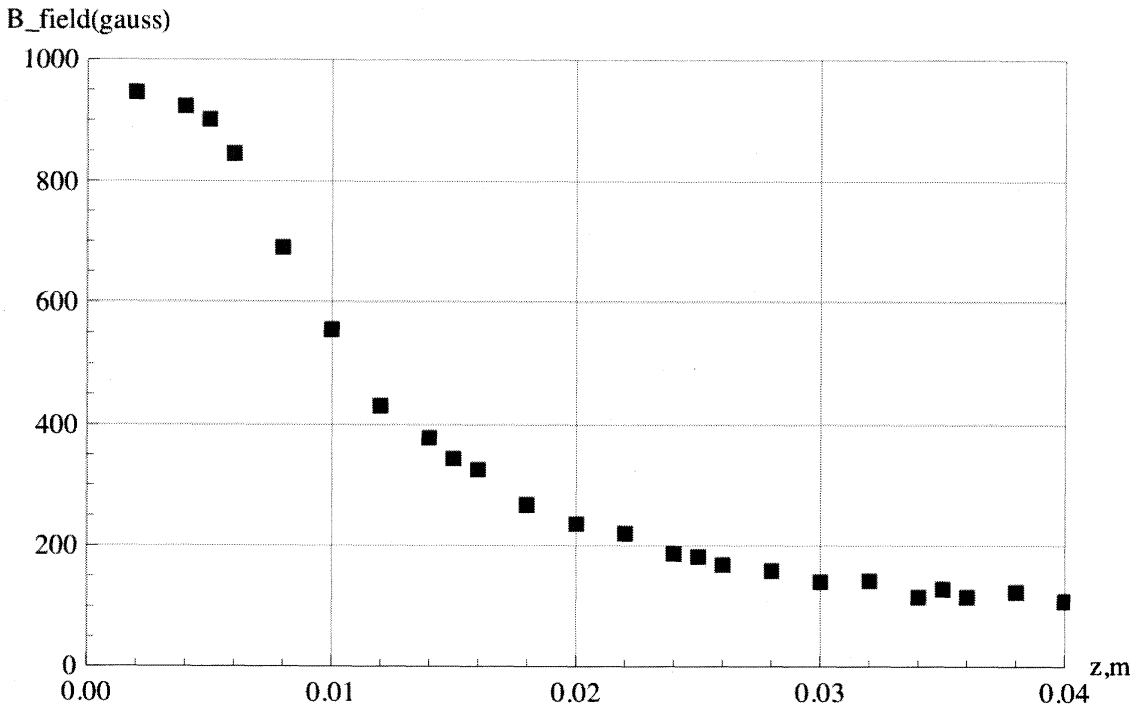

Figure 2. Magnetic field of a nut-shaped permanent magnet along the axial symmetry axis through the center of the magnet vs. distance.

```
dataNutmagnetDec16CGS = dataNutmagnetDec16 /. {p_, q_} → {100 (p(*(+6.5)/2*)), q}
```

```
{{0.2, {950}}, {0.4, {927}}, {0.5, {903, 908}}, {0.6, {835, 864}},
 {0.8, {678, 712, 688, 699}}, {1., {546, 561, 561, 551, 571}}, {1.2, {435}},
 {1.4, {395, 366, 383}}, {1.5, {348}}, {1.6, {327, 332}}, {1.8, {273, 270}},
 {2., {234, 234, 239, 241, 248}}, {2.2, {205, 224, 229, 234}}, {2.4, {177, 205}},
 {2.5, {185, 187}}, {2.6, {161, 170, 185}}, {2.8, {146, 156, 168, 177}},
 {3., {135, 141, 143, 148, 153}}, {3.2, {127, 151, 158}}, {3.4, {119}},
 {3.5, {133}}, {3.6, {114, 124}}, {3.8, {109, 131, 136, 138}},
 {4., {104, 109, 115, 115, 122}}, {4.6, {92}}, {5., {83, 114}}}
```

```
tabledataNutmagnetDec16CGS =
 Table[{dataNutmagnetDec16CGS[[i, 1]], Mean[dataNutmagnetDec16CGS[[i, 2]]] // N},
  {i, 1, Length[dataNutmagnetDec16CGS]}]
```

```
{{0.2, 950.}, {0.4, 927.}, {0.5, 905.5}, {0.6, 849.5}, {0.8, 694.25},
 {1., 558.}, {1.2, 435.}, {1.4, 381.333}, {1.5, 348.}, {1.6, 329.5},
 {1.8, 271.5}, {2., 239.2}, {2.2, 223.}, {2.4, 191.}, {2.5, 186.},
 {2.6, 172.}, {2.8, 161.75}, {3., 144.}, {3.2, 145.333}, {3.4, 119.},
 {3.5, 133.}, {3.6, 119.}, {3.8, 128.5}, {4., 113.}, {4.6, 92.}, {5., 98.5}}
```

3 Analysis

Assuming an electric current confined to a line is the source of the magnetic field, we utilize Biot-Saravt law evaluating the field [7].

$$\vec{B} = ik' \int \frac{d\vec{\ell} \times \vec{r}}{r^3} \tag{1}$$

In this equation, i is the curret and $k' = \frac{\mu_0}{4\pi}$; μ_0 is the permeability of vacuum and its value in MKS units is $k' = 10^{-7} \frac{T.m}{\text{Amp}}$, $d\vec{\ell}$ is the length element along the current i, $\vec{r}$ is the distance vector from the current element $i\,d\vec{\ell}$ to the point of interest where the magnetic field $\vec{B}$ is evaluated. A schematic of the setting is shown in Fig 3.

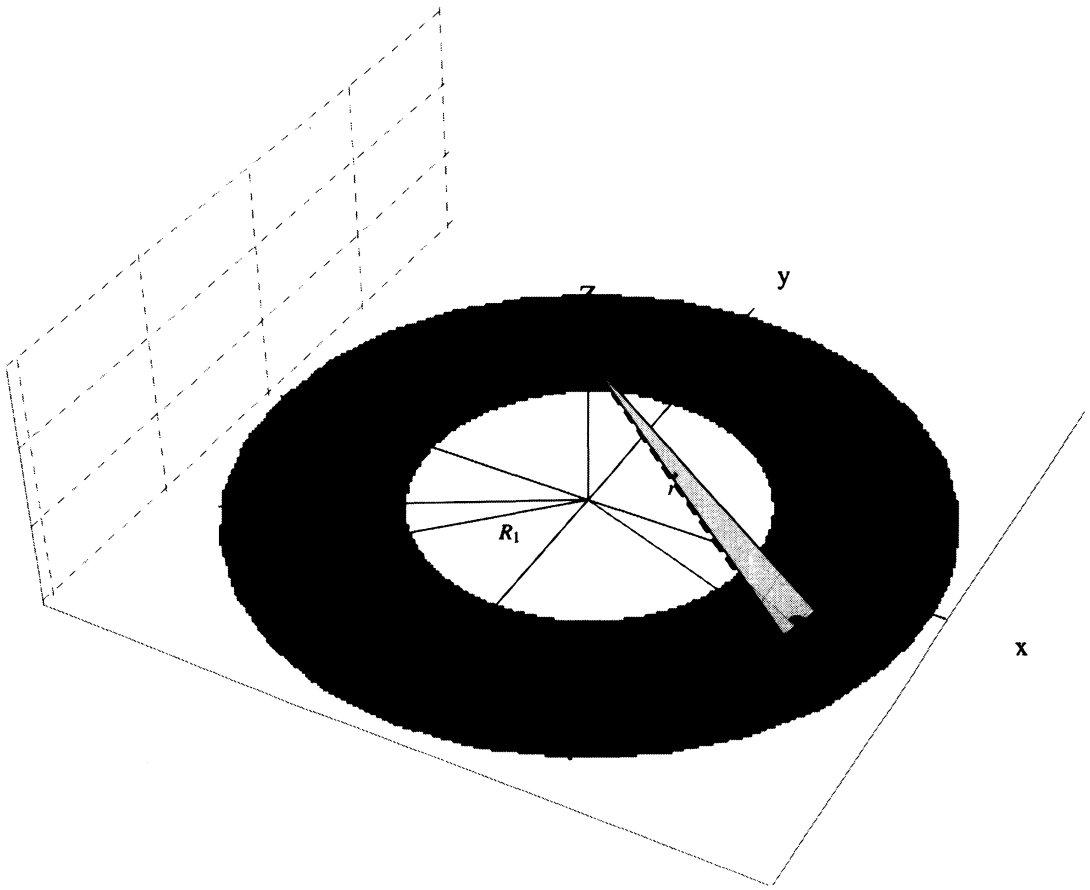

Figure 3. Display of a nut-shaped magnet with the inside and outside radii R_1 and R_2, respectively.

Assuming the current is distributed on the surface of the nut, the light grey ribbon shows a portion of the entire current i. The length element $d\vec{\ell}$, and the

position vector $\vec{r}$ are shown. The element of magnetic field $d\vec{B}$ due to current $i\, d\vec{\ell}$ is oriented perpendicular to the plane displayed by the yellow triangle formed with the side lengths of $d\vec{\ell}$ and $\vec{r}$ at a point of interest along the Z-axis is shown in blue.

For a nut-shaped permanent magnet and assumed surface current distribution shown in Fig 3, eqn (1), however, is to be modified. I.e., the current i is not confined to a thin circular loop around the vertical symmetry axis through the center of the nut, rather it is distributed over its surface. Denoting the current distribution density by $j = \frac{di}{da}$ where da is the surface element, i.e. the area of the light grey ribbon in Fig 3, eq (1) reads,

$$\vec{B} = k' \int j(\rho) da(\rho) \int \frac{d\vec{i} \times \vec{r}(\rho)}{r(\rho)^3} \tag{2}$$

here ρ is the radial parameter defining the geometry of the current distribution. The evenness of the current distribution about the symmetry axis about of the nut result a magnetic field along the z-axis only. We note,$d\ell = \rho d\varphi$ where φ is the polar angle and $\left(d\vec{\ell} \times \vec{r}\right)_z = (\rho d\varphi r)\cos\theta$ where θ is the angle between the orientation of the $d\vec{B}$ and the z-axis. Utilizing the geometry depicted in Fig 3, we replace $\cos\theta$ with $\sin\theta$ and we replace $\sin\theta$ with the relevant side lengths of the associated vertical triangle, namely $\sin\theta = \frac{\varrho}{r}$. Putting all this together eq (1) yields, $B(z) = k' \int \frac{\rho^2}{r^3} di\, d\varphi$. Moreover, since $di = j\, da$ and because $da = 2\pi\, \rho\, d\rho$ we arrive at, $B(z) = 2\pi k' \int j(\rho) \frac{\rho^3}{r^3} d\varphi\, d\rho$. From this point on one needs to make assumptions about the current distribution density j.

Model #1.

As a first intuitive model we assume the current is distributed evenly, and therefore its associated density is constant. With this assumption the latter integral yields,

$$B(z) = (2\pi)^2 k' j \int_{R_1}^{R_2} \frac{\rho^3}{\left(\rho^2 + z^2\right)^{\frac{3}{2}}} d\rho \tag{3}$$

where utilizing Fig 3 we substitute $r = \sqrt{\rho^2 + z^2}$. In eq (3) we replace the current density j in terms of its corresponding magnetic dipole moment μ. For a current looping in a line the magnetic moment is defined with $\mu = i\, A$, where A is the enclosed area by the loop. However, in our case study because the current is distributed over the surface of the nut we modify the moment accordingly; this yields $\mu = \int a\, di$. Replacing $di = j(\rho)\, da$ and the enclosed area with $a = \pi\, \rho^2$ the moment reads, $\mu = 2\pi^2 \int j(\rho)\rho^3 d\rho$. Applying the latter for the case at hand,

namely, a constant current density j, yields $\mu = 2\pi^2 j \int \rho^3 \, d\rho = \frac{\pi^2}{4} j(R_2^4 - R_1^4)$. We solve the last equation for j, and substitute its value in eq (3), integrating the function gives,

$$\left(\frac{B(z)}{\mu}\right)_{\text{nut}} = 8k' \frac{1}{R_2^4 - R_1^4} \left(\frac{2z^2 + R_2^2}{\sqrt{R_2^2 + z^2}} - \frac{2z^2 + R_1^2}{\sqrt{R_1^2 + z^2}} \right) \tag{4}$$

Since the moment μ is constant, we plot the left-hand side of eq (4) vs. distance z and compare the compatibility of the proposed current density hypothesis vs. collected data. Utilizing the specifications of the magnet on hand, namely, $\{R_2, R_1, t\} = \{1.0, 0.5, 0.3\}$ cm this is shown in Fig 4.

```
values = {R1 → 0.5 × 10^-2, R2 → 1.0 × 10^-2, kp → 10^-7};

BNutpermoment[z_] := 8 kp / (R2^4 - R1^4) (2 z^2 + R2^2)/Sqrt[R2^2 + z^2] - (2 z^2 + R1^2)/Sqrt[R1^2 + z^2]

Show[
 {ListPlot[Table[{dataNutmagnetDec16[[i, 1]], Mean[dataNutmagnetDec16[[i, 2]]] // N},
    {i, 1, Length[dataNutmagnetDec16]}], GridLines → Automatic, PlotMarkers → {■},
  PlotRange → {{0, 0.04}, {0, 1600}}, AxesLabel → {"z,m", "B_field(gauss)"}],
 Plot[200 + 3000 BNutpermoment[z] (*/.z→z-0.04*) /. values,
  {z, 0.000, 0.04}, PlotStyle → {Thick, Magenta}, GridLines → Automatic]}]
```

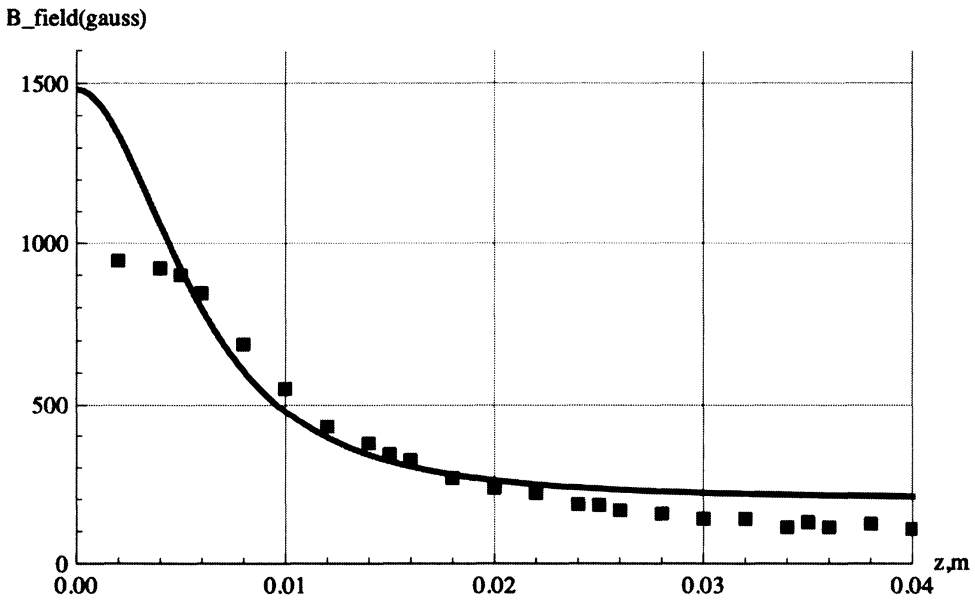

Figure 4. Magnetic field of the nut-shaped permanent magnet along the axial symmetry axis vs. distance from the center of the nut. Square marks are the data and the solid curve is theoretical field assuming the corresponding current has a constant density on the base of the nut.

The solid curve in Fig 4 is the plot of eq (4), however, the strength of the field for comparing to the data only was adjusted and its abscissa was shifted accordingly. We have not associated any physical meaning to these adjusted parameters yet. The trust of the procedure is to learn whether the proposed current distribution hypotheses is viable. According to Fig 4, for far and close distances the theory over estimates the data. Most important, at close distances the theory completely over estimates the data, and it appears there is a disjoint between the theory and data. From this unsuccessful model we propose a different hypothesis for the current distribution, the details follows.

Model #2.

In this model we assume the current has a non-uniform distribution. Intuitively one may assume the current density is in proportion to the surface area and its associated distance from the center of the nut. In other words, further the distance the larger the density. One may expand on this idea proposing nonlinear cases. For time being we assume a linear model such as $j(\rho) = a\,\rho + b$, where a and b are constants and are independent of distance ρ. We also assume the current densities at the inner and outer radii are: $j_1(R_1) \equiv \alpha\, j_0 = a\,R_1 + b$ and $j_2(R_2) \equiv \beta\, j_0 = a\,R_2 + b$ where the value of the constant current density $j_0 = \frac{i}{\pi(R_2^2 - R_1^2)}$. Solving these equations of a and b yields, $\{a, b\} = \left\{\left(\frac{\beta-\alpha}{R_2-R_1}\right) j_0, \left(\frac{aR_2-\beta R_1}{R_2-R_1}\right) j_0\right\}$. On the other hand $i = \int_{R_1}^{R_2} j(\rho)[2\pi\,\rho\,d\rho]$ substituting for $j(\rho) = a\,\rho + b$ and integrating over ρ yields, $i = 2\pi\left[\frac{1}{3}a(R_2^3 - R_1^3) + \frac{1}{2}b(R_2^2 - R_1^2)\right]$. Furthermore, by substituting in the latter the values of $\{a, b\}$ and j_0 gives,

$$\beta = \frac{1}{2R_2^2 - R_1(R_1+R_2)}\left\{3(R_2^2 - R_1^2) - \alpha\left[R_2(R_1 + R_2) - 2R_1^2\right]\right\}.$$

In other words, $\beta = \beta(\alpha)$. It is interesting to note that in the limit of $R_1 \to R_2$ the latter equation becomes independent of the radius and simplifies to $\beta = 2 - \alpha$ restricting the value of $\alpha = 1$. Utilizing the current density we may also calculate the magnetic moment of the magnet. Applying its expression from model #1, namely $\mu = 2\pi^2 \int j(\rho)\rho^3 d\,\rho$ yields, $\mu = 2\pi^2\left[\frac{1}{5}a(R_2^5 - R_1^5) + \frac{1}{4}b(R_2^4 - R_1^4)\right]$. Also as explained in the previous section magnetic field is $B(z) = 2\pi k' \int j(\rho)\frac{\rho^3}{r^3} d\,\varphi\, d\,\rho$. Utilizing this equation for the case in hand gives,

$$B(z) = (2\pi)^2 k'\left[a\int_{R_1}^{R_2} \frac{\rho^4}{(\rho^2+z^2)^{\frac{3}{2}}} d\,\rho + b\int_{R_1}^{R_2} \frac{\rho^3}{(\rho^2+z^2)^{\frac{3}{2}}} d\,\rho\right]$$

Generically speaking, since $\{a, b\} \sim j_0$ one may follow the procedure outlined in the previous section and by eliminating j_0 between the magnetic moment μ and $B(z)$ express the latter in terms of μ, this results a lengthy expression. However,

similar to eq (4), the ratio of $\left(\frac{B(z)}{\mu}\right)_{\text{nut}}$ becomes a function of distance z, which is also modified with an overall $\{R_1, R_2\}$ dependent function. Noticing the fact that the $\{R_1, R_2\}$ dependent multiplier factor is a scaling factor, for the purpose of current investigation it may be suppressed. Therefore, to illustrate the generic impact of the proposed current distribution we evaluate the $B(z)$ according to

$$B(z) \sim a \int_{R_1}^{R_2} \frac{\rho^4}{(\rho^2+z^2)^{\frac{3}{2}}} d\rho + b \int_{R_1}^{R_2} \frac{\rho^3}{(\rho^2+z^2)^{\frac{3}{2}}} d\rho \tag{5}$$

and the *Mathematica* codes are as follows,

```
intρ = {∫ ρ^4 dρ / (ρ^2 + z^2)^(3/2), ∫ ρ^3 dρ / (ρ^2 + z^2)^(3/2)};

{β, j0} = {1 / (2 R2^2 - R1 (R1 + R2)) (3 (R2^2 - R1^2) - α (R2 (R1 + R2) - 2 R1^2)), 1 / (π (R2^2 - R1^2))};

{a, b} = {((β - α) / (R2 - R1)) j0, ((α R2 - β R1) / (R2 - R1)) j0} // Simplify;
BNutρR2 = ((a intρ[[1]] + b intρ[[2]]) /. ρ → R2);
BNutρR1 = ((a intρ[[1]] + b intρ[[2]]) /. ρ → R1);
BNutρR1R2 = (BNutρR2 - BNutρR1) // Simplify
```

$$\frac{1}{2\pi\,(R1-R2)^2\,(R1+2\,R2)}$$

$$\left(-\left(2\left(R1^2+2\,z^2\right)\left(2\,R2^2\,\alpha+R1^2\,(-3+2\,\alpha)+R1\,R2\,(-3+2\,\alpha)\right)\right)\Big/\left((R1+R2)\sqrt{R1^2+z^2}\right)+\right.$$

$$\left(2\left(R2^2+2\,z^2\right)\left(2\,R2^2\,\alpha+R1^2\,(-3+2\,\alpha)+R1\,R2\,(-3+2\,\alpha)\right)\right)\Big/\left((R1+R2)\sqrt{R2^2+z^2}\right)+$$

$$3\,(-1+\alpha)\left(\frac{R1^3+3\,R1\,z^2}{\sqrt{R1^2+z^2}}-3\,z^2\,\text{Log}\left[2\left(R1+\sqrt{R1^2+z^2}\right)\right]\right)-$$

$$\left.3\,(-1+\alpha)\left(\frac{R2^3+3\,R2\,z^2}{\sqrt{R2^2+z^2}}-3\,z^2\,\text{Log}\left[2\left(R2+\sqrt{R2^2+z^2}\right)\right]\right)\right)$$

And for two values of a we display the associated fields vs. distance z.

```
GraphicsArray[{Show[{Plot[{BNutρR1R2 /. {R2 → 1.0, R1 → 0.5} /. α → 0.05,
      BNutρR1R2 /. {R2 → 1.0, R1 → 0.5} /. α → 1.9}, {z, 0, 3},
    PlotRange → {{0, 3}, {0, 0.25}}, AxesLabel → {"z,cm", "~B_field"},
    PlotStyle → {{Thick, Blue}, {Thick, Red}}, GridLines -> Automatic]}],
```

```
Plot[β /. {R2 → 1.0, R1 → 0.5} /. α → γ, {γ, 0, 2}, AxesLabel → {"α", "β"},
  PlotStyle → {Thick, Black}, GridLines → Automatic],
Plot[10^-6 (a ρ + b) /. values /. α → 0.2, {ρ, 0.5, 1},
  PlotRange → {{0, 1.5}, {0, 1.5}}, PlotStyle → {Thick, Black},
  AxesLabel → {"ρ,cm", "j(ρ),Amp/m²or ?? cm²"}, GridLines → Automatic]}
, ImageSize → 600]
```

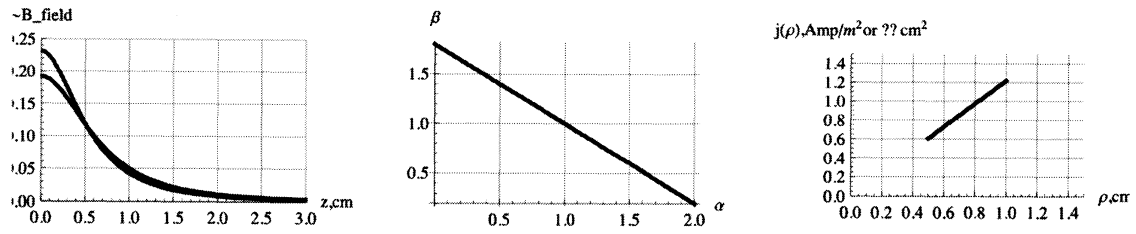

Figure 5. Magnetic field along the axial symmetry axis of the nut-shaped magnet vs. distance from the center of the nut. The black and grey curves correspond to values of $\alpha = 0.05$, and 1.9, respectively (left graph). The middle graph is the display of the parameter β vs. α. A plot of a typical e.g.$\alpha = 0.5$ linearly increasing current density distribution function vs. radial distance ρ (the right graph).

Plots displayed in Fig 5 are interpreted as follows. According to the left graph, the tails of the magnetic fields for distances far from the magnet irrespective the values of α and β, i.e. the character of the current distributions are indistinguishably identical. One needs to recall according to $j_1(R_1) = \alpha j_0$ and $j_2(R_2) = \beta j_0$ the values of α and β are the factors determining the portion of the entire currents that runs in the inner and the outer circumference of the nut. The overlapping tails of the fields at far distances, therefore, means, knowing the current distribution is irrelevant. This is not true for close distances. The blue curve corresponds to a small a and the red curve corresponds to a large α, respectively. We have compared these two curves vs. data, but not shown in this report. However, it is obvious that the curve with a small α favors the data. On the other hand, according to the middle graph of Fig 5, the small value of a corresponds to a large value of β. And because β is the factor that determines the portion of the current that runs in the outer edge, we then conclude [to make the current distribution model conducive to the measured field, the current on the surface of the nut needs a higher concentration at the outer edge]. Graphically this is depicted by the right most graph of Fig 5. In short, by implementing Model #2 we learned the current on the base surface of the nut is not distributed evenly. Moreover, a steeper linear increment is favored. With these insights we propose the next model.

Model #3.

Guided with the outcome of Model #2, we propose our upgraded model. In this

model the current is concentrated only on the rim of the outer radius of the nut. For this simple situation eq (1) gives, $B(z) = 2k' \frac{\mu}{(R^2+z^2)^{\frac{3}{2}}}$, where the magnetic moment is $\mu = (\pi R^2)\, i$. We refer the field as field_ring. Utilizing the specifications of the nut, we plot the last expression, $\left(\frac{\text{field}}{\mu}\right)_{\text{Ring}}$,

```
values =

{R1 → 0.005, R2 → 0.01, kp → 1/10 000 000}

BRingpermoment[z_] := 2 kp / (R2^2 + z^2)^(3/2)

Show[
 {ListPlot[Table[{dataNutmagnetDec16[[i, 1]], Mean[dataNutmagnetDec16[[i, 2]]] // N},
    {i, 1, Length[dataNutmagnetDec16]}], GridLines → Automatic,
  PlotMarkers → {■}, PlotRange → {{0, 0.04}, {0, 1400}}],
 Plot[125 + 5700 BRingpermoment[z] /. values, {z, 0.001, 5 R2 /. values},
  PlotRange → All, AxesLabel → {"z,m", "gauss/moment"}, PlotStyle → Thick,
  PlotLabel → "Ring"]}, AxesLabel → {"z,m", "B_field/μ"}]
```

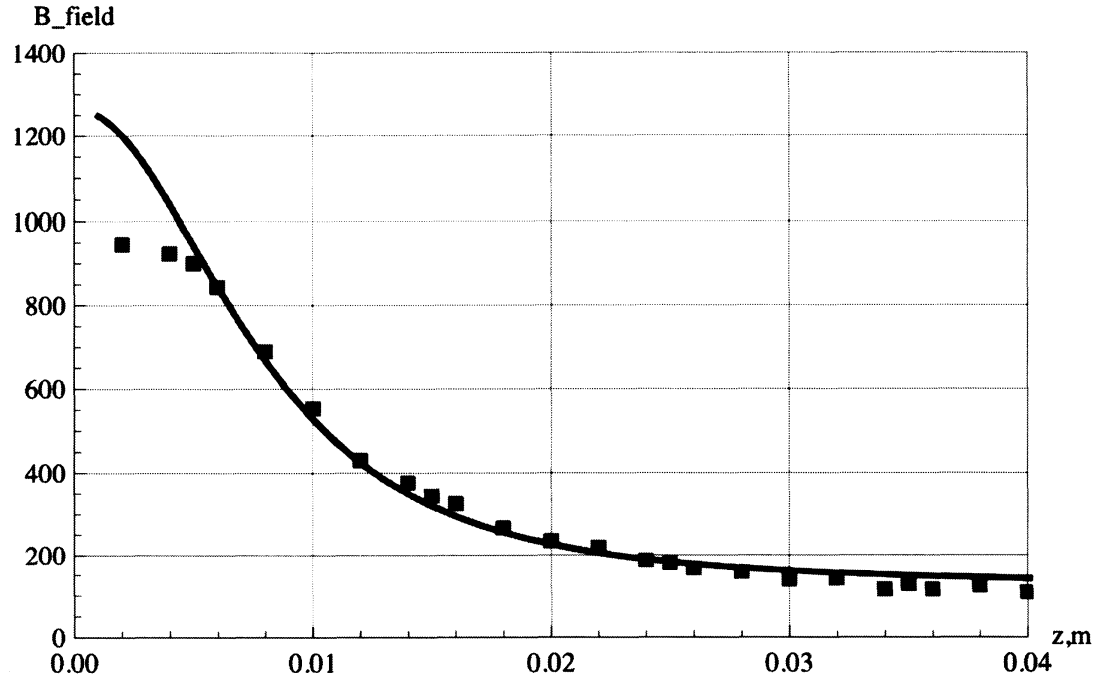

Figure 6. Magnetic field of a nut-shaped magnet along the axial symmetry axis through the center of the nut. The curve is due to current distribution confined to the outer circumference of the nut. The filled squares is the data.

Figure 6 shows Model #3 works the best. For distances far from the magnet the theory matches perfectly with data. For close distances the theoretical model

curve over weighs the data. Comparing Fig 6 vs. Fig 4 we see a great deal of improvement. Meaning, by concentrating the current to the outer rim of the nut the agreement between the data and theory improves. Encouraged with this result, we adjust the model.

Model #4.

Building on the descriptive conclusions of Model #3, here we propose a current distribution that is partially stretched beyond the outer rim of the nut. One may think of the similarity of the proposed current to the notion of Maxwell's displaced current [7]. The latter comes about from time variation of the electric field, here, the "displaced" current comes about from stretching the conduction current beyond the physical dimension of the nut. We assume a current density such as:

$$j(\rho) = \begin{cases} 0 & 0 \leqq \rho < R_2 \\ \frac{i}{N} e^{-\lambda \rho} & \rho \geqq R_2 \end{cases} \tag{6}$$

where λ is is the decay constant of the current and N is the normalization factor. Utilizing $j = \frac{di}{d\alpha}$ we determine the normalization factor accordingly, namely $i = \int_0^\infty j(\rho)[2\pi\,\rho\, d\,\rho] = \frac{i}{N}\int_{R_2}^\infty e^{-\lambda\rho}[2\pi\,\rho\, d\,\rho]$. The actual outer radius of the nut is $R_2 = 1$cm this yields, $N = 2\pi e^{-\lambda}\frac{(1+\lambda)}{\lambda^2}$. As expected the normalization factor is $N = N(\lambda)$. We insert the current distribution in the recipe of the magnetic field, namely, $B(z) = 2\pi k' \int j(\rho)\frac{\rho^3}{r^3} d\varphi\, d\,\rho$, this gives

$$B(z) = ik'(2\pi)^2 \int_{R_2}^\infty \frac{e^{-\lambda p}}{N(\lambda)} \frac{\rho^3}{(\rho^2 + z^2)^{\frac{3}{2}}} d\,\rho \tag{7}$$

For the sake of coding only, we replace N with A1, and compose a code allowing to plot the field for various values of λ this is shown in Fig 7.

```
A1 = 2 π Integrate[ρ e^(-λ ρ), {ρ, 1, ∞}, Assumptions → Re[λ] > 0];

j1[ρ_] = 1/A1 e^(-λ ρ);

tabplotBλ =
  Table[Plot[65.8 + 221 (2 π)^2 NIntegrate[j1[ρ] ρ^3/(ρ^2 + (z(*-0.4*))^2)^(3/2), {ρ, 1.0, 3.0}],
    {z, 0.15, 5}, PlotStyle → {Thick, Hue[0.2 λ]},
    AxesLabel → {"z,cm", "B_field(gauss)"}, PlotRange → {{0, 5}, {0, 1200}},
    GridLines → Automatic], {λ, 2.0, 3.0, 0.5}];

Show[{tabplotBλ[[1]], tabplotBλ[[2]], tabplotBλ[[3]]}];
```

```
listplotdataNutmagnetDec16CGS = ListPlot[
    Table[{dataNutmagnetDec16CGS[[i, 1]], Mean[dataNutmagnetDec16CGS[[i, 2]]] // N},
     {i, 1, Length[dataNutmagnetDec16CGS]}], GridLines → Automatic,
    PlotMarkers → {■}, PlotRange → {{0, 5.0}, {0, 1000}},
    AxesLabel → {"x(cm)", "B_field(gauss)"}];

Show[{Flatten[Table[tabplotBλ[[n]], {n, 1, Length[tabplotBλ]}]], (*,
  tabplotB[[1]]*)listplotdataNutmagnetDec16CGS}, GridLines → Automatic]
```

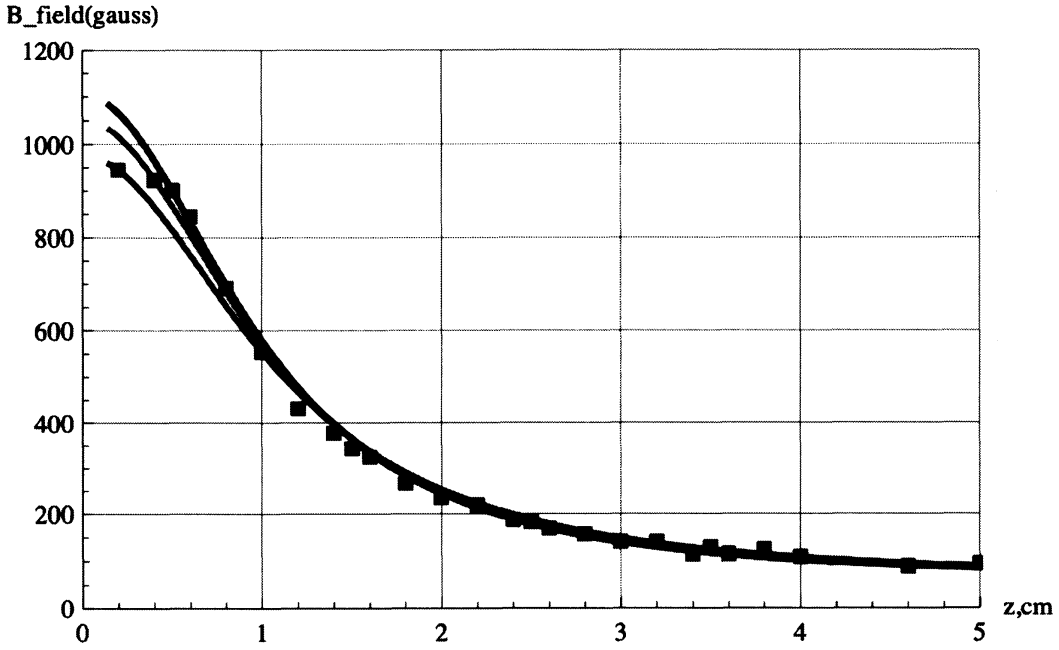

Figure 7. The curves are associated with the *halo* currents. The weakest field (the grey curve) corresponds to $\lambda = 2.0$ and the strongest field (the black curve) corresponds to $\lambda = 3.0$, respectively. The middle curve (the light grey) has a values of $\lambda = 2.5$.

According to Fig 7, the *halo* currents with decay parameters within the range of $2 \leqq \lambda \leqq 3$ produce magnetic fields that are most compatible with data. The most important feature of the *halo* current is its corresponding field at close distances to the magnet. Comparing to Fig 4 and 6 the strength of the fields vs. Fig 7 does not over estimate the data and bents according to what data indicates. Also we notice at distances far from the magnet, say beyond 0.8 cm the *halo*'s current decay constant, λ appears to be insignificant; all three curves overlap. For a comprehensive visualization purpose in Fig 8 we have shown a 3D plot of the current density distributions in accordance to what we discussed in four models.

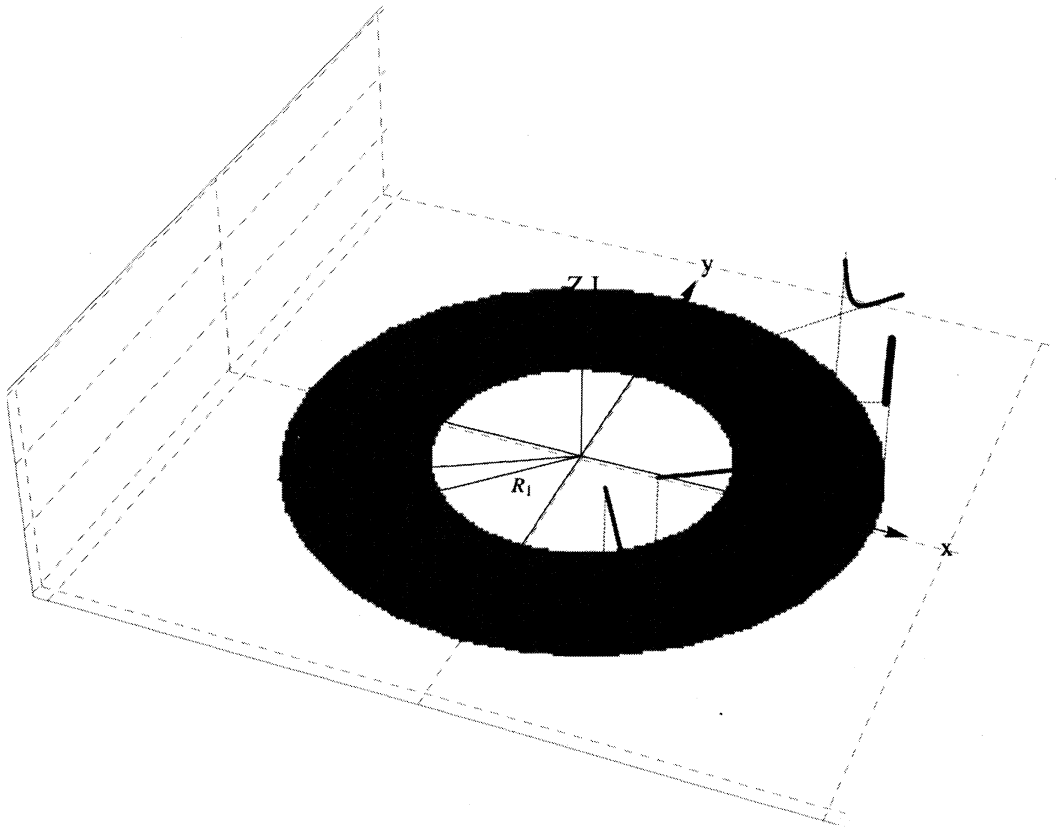

Figure 8. A 3D plot of the current distribution densities corresponding to models 1-4. Beginning with the fourth quadrant and in counterclockwise direction, each grey line/curve corresponds to Model #1-4, respectively.

4 Conclusions

In the course of our investigation we stumbled upon a nut-shaped permanent magnet. Utilizing a popular magnetometer we measure the strength of its magnetic field along its axial symmetry axis through the center and perpendicular the center of the nut. In order to interpret the data we assume the electric current is the source of the field. We begin our analysis with modeling the current distributions. From the short coming of the models we systematically upgrade our thoughts. Each upgrade improved the previous model and after four attempts we were able to propose a fresh idea, namely the existence of a *halo* current; it enables to producing results compatible with data. The notion of extending the conduction current beyond the physical dimension of a permanent magnet is innovative and fresh. A thorough scientific literature search reveals no such idea has been considered before. This article also emphasizes the fact that physics is an empirical science and data guides the theoretical modeling.

Acknowledgement

The author would like to thank the Research Institute for Mathematical Sciences of Kyoto University for its financial support so he could attend the RIMS Symposium and present this work.

References

[1] H. Sarafian, Dynamic Dipole-dipole Magnetic Interaction and Damped Nonlinear Oscillations, Journal of Electromagnetic Analysis and Applications, 2009, 1: 195-204

[2] www.allelectronics.com

[3] Pasco^{Tm} Magnetic Field Sensor/Gauss meter, CI-6520

[4] Pasco^{Tm} ScienceWorkshop 750 Interface

[5] Pasco^{Tm} DataStudio software

[6] S. Wolfram, "The Mathematica Book," 5th ed., Cambridge University Publications, 2003; Mathematica, V7.01

[7] E.g. J.D. Jackson, "Classical Electrodynamics," 3rd ed., Wiley, 2005